ISSN: 2229-6956 (ONLINE)
DOI: 10.21917/ijsc.2021.0322

BLOCK WISE 3D PALMPRINT RECOGNITION BASED ON TAN AND TRIGGS WITH BSIF DESCRIPTOR

Nour Elhouda Chalabi, Abdelouahab Attia and Abderraouf Bouziane
[1,3]*Department of Computer Science, Mohamed El Bachir El Ibrahimi University of Bordj Bou Arreridj, Algeria*
[2]*LMSE Laboratory, Mohamed El Bachir El Ibrahimi University of Bordj Bou Arreridj, Algeria*

Abstract

Faced by problems such as lack of robustness from 2D palmprint recognition system which can result to be attacked using a fake palmprint or having the same palmprint as another individual, 3D can present an alternative solution to deal with this problem, hence in this paper we are going to introduce a novel approach based on 3D palmprint recognition system named TT-P-BSIF: first, a preprocessing technique based on Tan and Triggs method was applied on a 3D depth image in order to effectively and efficiently eliminate the effect of low frequency component and at the same time keeping the local statistical properties of the treated image. Then the processed image is divided into a regular number of blocks using two parameters (a and b), after that the Binarized Statistical local features (BSIF) has been applied on each block in order to extract the features vector. These vectors are all combined to produce one larger vector for each processed image. Afterwards nearest neighbor classifier is used to classifier the 3D palmprint images. To examine the proposed method, this latter has been evaluated on a 3D palmprint database that contains 8,000 samples, the obtained results were consistent and promising which proves that the introduced method can massively and effectively improve the recognition results. Therefore, this proposed work using Tan and Triggs method for preprocessing and BSIF for feature extraction was able to generate a recognition rate up to 99.63% and verification rate at 1% up to 100% with EER equals to 0.12%.

Keywords:

3D Palmprint, Tan and Triggs, BSIF, Nearest Neighbor Classifier

1. INTRODUCTION

Biometrics, yet one of the most powerful technologies used to fulfill security-related requisites.[1] Over the years and until now, different biometrics have been designed effectively where it uses behavioral characteristics and / or physiological specific to each person due to its advantages such as universality, uniqueness and durability counter to some traditional means like password or badges[2]. Thus, a variety of biometric techniques have been introduced and used in the industries based on several biometric trait such as: palmprint, fingerprint, face, hand, iris, voice, and signature [2]–[4], 3D palmprint is no exemption, this latter was introduced to the recognition problems in order to overcome some of the limitation set previously by other modalities as 3D palmprint is considered very promising given that the availability of the 3D acquisition devices.[5] Despite some of the drawbacks of 3D palmprint approaches such as the long computation time required and the lack of robustness it still very useful as the 3D recognition model can retain all the information needed on the palmprint geometry which provides a real representation of the latter. However, several methods have been introduced to counter and face those drawbacks and challenges. Many works in the literature has been conducted until now using 3D palmprint Zhang et al. [6] were the first to explore the use of 3D palmprint recognition system by exploiting the 3D palmprint structural information by extracting features such as the Mean Curvature Image (MCI), Gaussian Curvature Image (GCI) and Surface Type (ST) features, those features have been used since. Zhang et al. [7] proposed a multimodal system using both 2D and 3D palmprint, after the localization of the ROI for each image separately and accordingly, the authors used Gabor features to extract the features for the 2D images and surface curvature features for 3D images as for the matching they applied local correlation (LC) for 3D images and Angular matching as for 2D images, lastly a score level fusion was done after the evaluation of 3D palmprint images if the 3D palmprint pass the decision phase then the fusion with 2D is proceeded to make the final decision. In another work Cui [8] has proposed a yet another multimodal recognition system based on 2D and 3D palmprint images in order to boost the accuracy, the author used principal component analysis (PCA) to extract the features from both traits after that we use two-phase test sample representation (TPTSR) was employed on each trait separately finally a fusion module was used on the matching score. Zhang et al. [9] presented 3D palmprint identification based on block-wise method with collaborative representation (CR) and using l1-norm or l2-norm regularizations, the authors used specific schema for feature extraction where he divided the image of 3D palmprint into regular blocks in order to make the system more robust. Yang et al. [10] used block-wise method in a multi-dictionary Based Collaborative Representation for 3D palmprint 3D ear where they divided the image into blocks then compute reconstruction residuals for each block using CR and lastly fuse the residuals in order to predict the class label. Meraoumia et al. [11] proposed in another work a multimodal 2D and 3D palmprint recognition system based on score level fusion and feature extraction level fusion. The authors used Principal Component Analysis (PCA) for feature extraction and dimensionality reduction on each modality, also used Hidden Markov Model (HMM) for modeling the feature vector and for the evaluation Log-likelihood. Chaa et al. [12] presented a multimodal of 2D and 3D palmprint recognition system based score level fusion, were binarized statistical image features (BSIF) for feature extraction, note that all the different size and length of the descriptor where used and the resulting vectors where concatenated in one big vector for each image, and PCA as well as LDA methods were used for dimensionality reduction as for the matching phase the cosine Mahalanobis distance was employed.

Recently several papers has introduced systems based on 3D palmprint. However, in 2016 Bai et al. [13] draw a biometric system for person authentication using 3D palmprint data. This system is based on several Gabor filters to extract the orientation features of 3D palmprint image, in 2017 Yang et al. [14] published a paper for 3D palmprint recognition by using shape index image and fragile bits. Also, Chaa et al. [15] have introduced 3D

palmprint recognition structure based on an unsupervised convolutional deep learning network known as PCANet. Particularly, the framework first extract illumination-invariant 3D palmprint images by the Single Scale Retinex (SSR) method. Then, PCANet technique is used to extract discriminative features from SSR features. Finally, a multi-class support vector machine (SVM) classification is employed to identify the identity of the individual. Lunke et al. [16] investigated the precision direction code combined with compact surface type (PDCST) technique which applied for 3D palmprint representation and identification. Xuefei et al. [17] proposed a paper which described a novel 3D palmprint identification method by the mean of using blocked histogram feature (BHF) and improved sparse representation-based classifier (SRC).

The main contributions of this paper are: (1) it uses Tan and triggs in the preprocessing step to enhanced 3D palmprint images; and (2) split TT images in set of block; and (3) we apply BSIF descriptor on each block to extract BSIF histogram; followed by combining all histograms to create one large vector of every TT image;(4); finally the matching process in order to make a decision.

The rest of the paper is organized as follows: section two is going to focus on the proposed method including the preprocessing technique and the feature extraction method used. Section three focus on the experiments conducted and the discussion of the obtained results. Finally, section four is a conclusion.

2. PROPOSED METHOD

The Fig.1 describe the general architecture of the proposed system and it main steps including BSIF and cosine nearest neighbor classifier for classification.

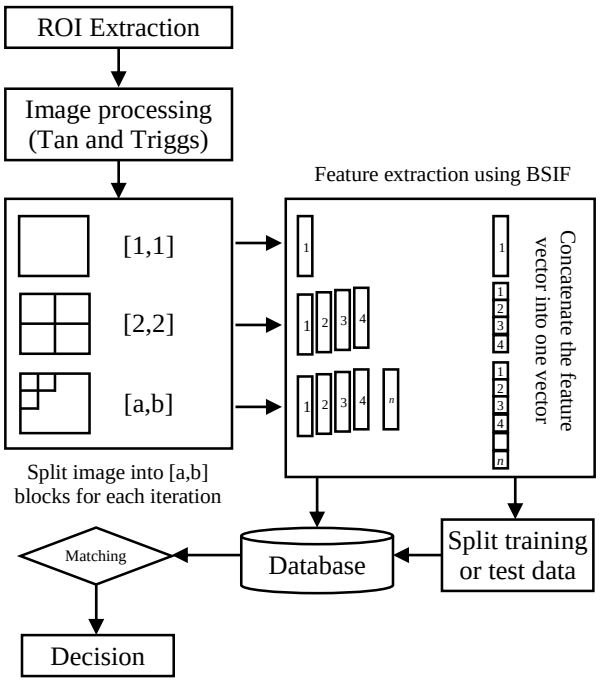

Fig.1. Schema of the proposed method

As despite in Fig.1 our proposed system contain four important steps which are region of interest (ROI) extraction from the 3D palmprint images, followed by a pre-processing using Tan and Triggs method, a block-wise division where we split the image into a regular number of blocks we denote that the main aim for using blocks is to insure the extraction of all the relevant features within the image which leads us to the feature extraction step, here we employed Binarized Statistical Image Feature (BSIF) descriptor then what results from the previous step is going to be fed the matching module to finally make a decision.

2.1 REGION OF INTEREST EXTRACTION

This sub-section describes the process of region of interest (ROI) extraction for 3D palmprint images. First a CCD camera was used in order to capture the image of 2D palmprint. Afterwards the process for ROI extraction starts as it can be seen Fig.2 during the first phase a Gaussian smoothing operation has been applied to the input image then followed by a binarization for the smoothed image using a threshold H as shown in Fig.2(a) and Fig.2(b). Once the binarization is done the boundaries of the binary image are extracted by applying a boundary tracking algorithm as in Fig.2(c). Then the points P_1 and P_2 were determinated to locate the 2D ROI pattern of the boundary image. As results the ROI system has been extracted, the region of the ROI has been located by the rectangle as in Fig.2(d). The extracted 2D ROI is shown in Fig.2(e). The Fig.2(f) represent the 3D palmprint image, while Fig.2(g) illustrates the obtained 3D ROI by jointing the cloud points corresponding to the pixels in 2D ROI as introduced in [8].

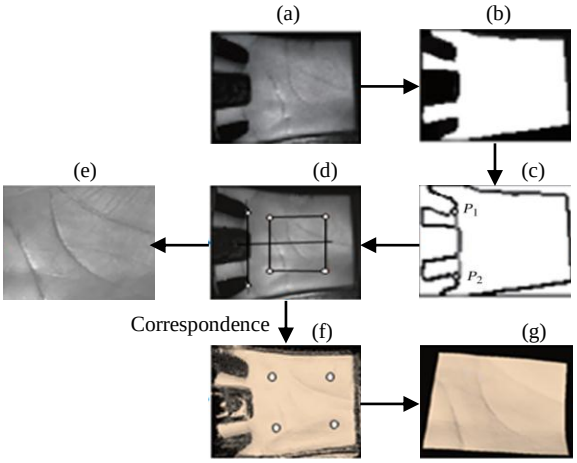

Fig.2. Steps of extraction ROI of 3D palmprint image.

2.2 TAN AND TRIGGS PREPROCESSING (TT)

TT [16] was first introduced for face recognition as an illumination preprocessing method in order to overcome the illumination variations, this preprocessing method includes a series of steps such as Gamma correction, Difference of Gaussians, Contrast equalization which are the main steps.

- ***Gamma Correction:*** This first step is simply described by the first mathematical equation:

$$I'(i,j) = I(i,j)^{\tau} \text{ where } \tau \in [0,1] \quad (1)$$

where $I(i,j)$ is the input image and $I'(i,j)$ is the image resulting from this first step of preprocessing. Here τ are stands for the gamma value.

- ***Difference of Gaussians:*** As in the first step Gamma correction is not able to remove the influence of overall intensity gradients. So in this second step Difference of Gaussians is used and it consist of the implementation of a band pass to remove low frequencies containing the undesirable effects of shadows and high frequencies containing aliasing and noise.
- ***Contrast Equalization:*** This last step is carried out of 3 steps process as follows:

$$I(i,j) = \frac{I(i,j)}{\left(mean\left(\left|I(i',j')\right|^{\alpha}\right)\right)^{\frac{1}{\alpha}}} \quad (2)$$

$$I(i,j) = \frac{I(i,j)}{\left(mean\left(min\left(\rho,\left|I(i',j')\right|^{\alpha}\right)\right)\right)^{\frac{1}{\alpha}}} \quad (3)$$

$$I(i,j) = \rho \tanh\left(\frac{I(i,j)}{\rho}\right) \quad (4)$$

where, α is a strongly compressive exponent that reduces the influence of large values, ρ is a threshold used to truncate large values after the first phase of normalization, and the mean is over the whole (unmasked part of the) image. The results obtained from the above steps is an image with pixel intensity in the range $(-\rho, \rho)$. The Fig.3 shows the before and after preprocessing image.

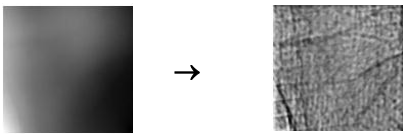

Before Preprocessing | After Preprocessing

Fig.3. 3D palmprint image before and after Tan and Triggs preprocessing

2.3 BLOCK DIVISION

At this stage a division of the image is done using a split function, this latter uses two parameters number of rows and number of columns in order to divide the image into a regular number of sub-images or blocks as illustrated in Fig.4, the aim behind this step is to insure a max spread of feature extraction from all the image. Note that as the number of rows and columns increase implicate the augmentation in the number of blocks.

2.4 FEATURE EXTRACTION

As known feature extraction stage is a very important phase in any recognition system as the final results of the classification depends on it. Here the feature extraction method used is Binarized Statistical Image Feature (BSIF) descriptor [17]. Hence, BSIF descriptor prove its effectiveness [19] [20]. Is a recently presented textural local descriptor. It uses a set of filters with a fixed size that describes the neighbourhood configuration of the central pixel. After the BSIF set filters $\varphi_i^{x\times k}$ are given an image X of size $m\times n$ the responses are binarized. The filter results is obtained as follows [17]:

$$r_i = \sum_{m,n} \varphi_i^{kxk} X(m,n) \quad (5)$$

Here, $\varphi_i^{x\times k}$ is a linear filter of size k and $i=\{1,2,\ldots,n\}$ denotes the number of statistically independent filters whose response can be computed together and binarized to obtain the binary string as follows [21]:

$$b_i = \begin{cases} 1 & \text{if } r_i > 0 \\ 0 & \text{otherwise} \end{cases} \quad (6)$$

Once the binarization is done, the BSIF features then are obtained as the histogram of pixel's binary codes that can effectively characterize the texture components in the image. We note that there are two important factors in BSIF descriptor namely: the filter size k and the filter length (n).

After the division of the image into blocks, BSIF was applied on each block to extract the features then the obtained features vectors of each image were concatenated to obtain one vector for each image to then feed it to the classifier.

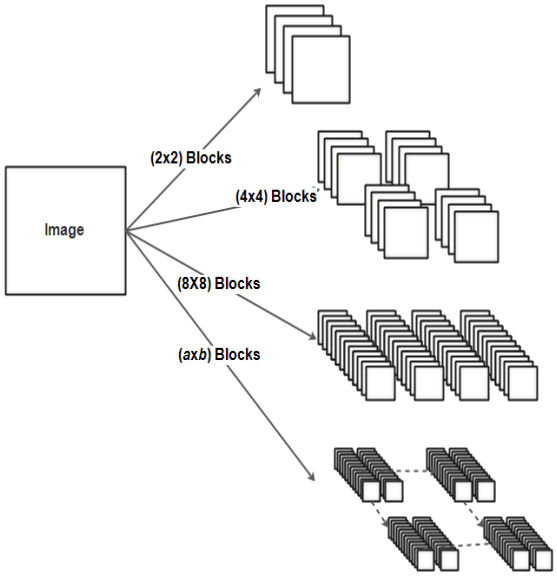

Fig.4. Illustration of the image division step

2.5 DIMENSIONALITY REDUCTION

The previous step feature extraction provide feature vectors of high dimension which are very difficult to use by the classification algorithm. That's why, to solve the problem of these large data, the techniques PCA+LDA dimensionality reduction has been used. The PCA+LDA method is one of the best techniques which is fast and simple, The PCA is first used to project the images into a lower data space [22]. The goal of the LDA is to maximize inter-class distances while minimizing intra-class distances, which amounts to finding the matrix of transformation W which maximizes criterion [23]:

$$T(W) = W_{opt} = \arg\max_{W} \frac{\left|W^T S_B W\right|}{\left|W^T S_W W\right|} = \left[W_1 W_2, \ldots, W_d\right] \quad (7)$$

where, $T(W)$ is the fisher discriminant criterion, that is maximized, W is built by concatenation of the number d leading Eigenvectors. Note that W is obtained by resolving the following system:

$$S_W^{-1} S_B W_j = W_j \lambda_j \quad (8)$$

where, j=1,2,…,d Applying the PCA+LDA method on the selected data, 399 most important features have been selected for 3D palmprint database.

2.6 MATCHING MODULE

In the matching module, nearest neighbor has been applied as a classifier for all test images, this latter uses the Mehalanobis distance to operate. Assume that, two vectors V_i and V_j characterize the feature vectors of query and images stored in database respectively. The distance between V_i and V_j has been calculated by the following equation:

$$d_{Ma}(V_i,V_j) = (V_i\text{-}V_j)^T C^{-1}(V_i\text{-}V_j) \quad (9)$$

In the above equation, C represents the covariance matrix.

3. EXPERIMENT RESULTS

3.1 DATABASE

The database used for this experiment in this work is a 3D or 2D ROI palmprint data base collected by Hong Kong polytechnic university (PolyU) [21], it contains 400 classes. In our work we used 8.0000 images and each class was represented by 20 images. The first 10 images were used for training while the other 10 images were used for test. Matlab R2017 and Windows 10 operating system were used to test the introduced method.

3.2 3D PALMPRINT EXPERIMENT

In this section we present and discus the experiment that was carried out. We have explored all BSIF filter and used different image division blocks (4 and 16). The aim of this experiment is to boost the performance of the system (accuracy) by constructing a bank of filters. In order to find the best filter and it parameters as well as the best number of blocks, we conducted several experiments and the results are reported in Table.1 - Table.6. We have explored in those experiments different parameters (filter size (k) and filter length (n)) and division of the image into different number of block number. Note that the experiment was carried out in three different sub experiment in order to be able to clearly see and compare the results since the BSIF descriptor contains a variety of filter sizes as well as filter length in addition to our block wise division that we propose.

In the first experiment we see the first lower filters sizes which are 3, 5, 7 and 9 with a filter length of 8 and number block equals to 16, note that the purposes for choosing those parameters is that a lower filter length to 8 don't give good results meanwhile any higher is computationally too expensive as for the number of blocks we did choose 16 since 4 blocks does not present good results.

In the second experiment we see filters 11, 13 and 15 with filter length 8 and different block number (4 and 16) same for the choice of filter length any lower don't present good results any higher is computationally too expensive.

For the last experiment it was carried on the last filter size which is 17 the higher one with filter lengths 8, 9, 10, 11 and 12 in order to see the changes and the differences in case of filter length change and with block division of 4 and 16.

Finally, an additional experiment was done with a full image with same filter size and length in order to carry out a comparative study and see the differences in case of using a block division and without block division.

3.2.1 Experiment I:

The results are introduced in Table.1.

Table.1. Accuracy and recognition rate for the filters size 3, 5, 7 and 9 with 16 blocks per image

BSIF filter size		Number of Block	Identification	Verification	
			Rank-one	V@1 %	EER %
k	***n***				
3×3	8	4×4	91.90%	96.78%	2.24%
5×5	8	4×4	93.92%	97.90%	1.55%
7×7	8	4×4	95.73%	98.40%	1.35%
9×9	8	4×4	97.15%	99.02%	0.98%

The Table.1 represent the results of the BSIF descriptor of the filters with a size 3, 5, 7 and 9 which are the smallest alongside a filter length of 8 and number of blocks equals to 16 blocks per image. From Table. we can observe that the higher the filter size is the better the results are where it varies from 91.90% for the accuracy at Rank one and an EER that equals to 2.24% and a verification accuracy at 1% of 96.78% where those results belong to the filter size 3 to the higher filter size which is in this case filter size 9, where this latter gives the best results in regard to accuracy at Rank-one with 97.15% and an EER that equals to 0.98% and a verification accuracy at 1% equals to 99.02 which is considered a good results in comparison with the other filters 3, 5, 7 and using a block division of 16 blocks per image.

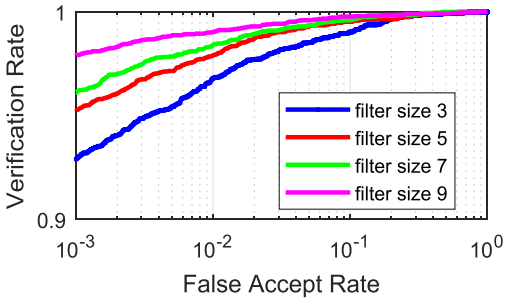

(a)

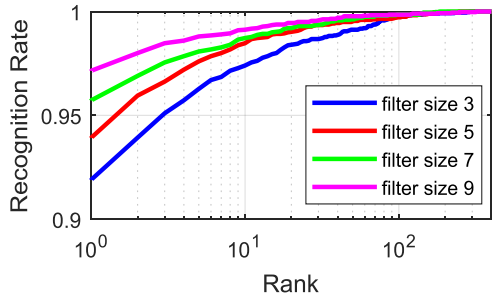

(b)

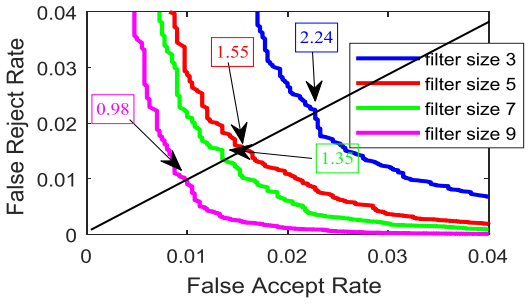

(c)

Fig.5. Results of 3, 5, 7 and 9 BSIF filters: (a) ROC (b) CMC (c) EER

In order to expand our findings, the results are represented in terms of ROC, CMC and EER curves which can be seen in Fig.5 where this latter delivers a comparison study between the filters size 3, 5, 7 and 9 results with a filter length of 8 and number of blocks equals to 16. It can be seen clearly from the Fig.5 that the BSIF filter number 9 perform better in comparison to the other lower filters when the filter length is equal to 8 and the number blocks is 16.

3.2.2 Experiment II:

The results are introduced in Table.2 for 4 blocks per image, while Table.3 introduce the results for 16 blocks per image.

Table.2. Accuracy and recognition rate for the filters size 11, 13, and 15 with 4 blocks per image

BSIF filter size		**Number of Block *a*×*b***	**Identification**	**Verification**	
K	***n***		**Rank-one**	**V@1 %**	**EER %**
11×11	8	2×2	80.33%	90.38%	4.31%
13×13	8	2×2	87.72%	94.95%	2.91%
15×15	8	2×2	92.88%	97.03%	1.95%

From Table.2 which present the results for the BSIF descriptor for filters size 11, 13 and 15 with filter length 8 and division of 4 blocks per image, it can be seen that the filter size 15 gives the best results in comparison to the other two with an accuracy at Rank-one of 92.88% while the other two give 80.33% and 87.72% and verification accuracy at 1% with 97.03% while the others give 90.38% and 94.95% as for the EER it can clearly be seen that the best which is 1.95% belongs to the filter size 15 as for the others two they gives 4.31% 2.91% however the given results do not outperform the results obtained from the previous experiment since in this experiment we use a block division of 4 blocks per image while in the previous experiment it uses a 16 block per image despite the fact that the filter of the pervious experiment belongs to the lower range.

The Fig.6 represent the results in terms of ROC, CMC and EER curves where this latter delivers a comparison study between the filters size 11, 13, and 15 results with a filter length of 8 and number of blocks equals to 4. It can be seen clearly from the Fig.6 that the BSIF filter number 15 perform better in comparison to the other filters.

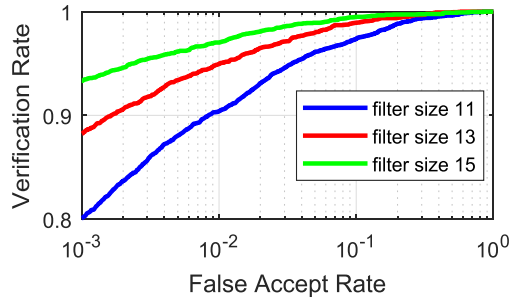

(a)

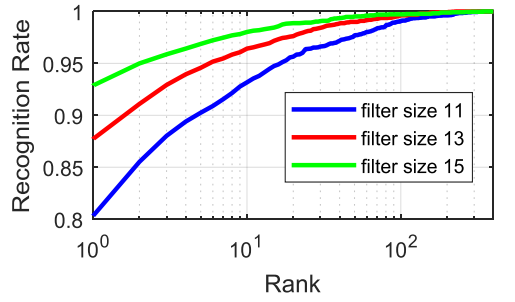

(b)

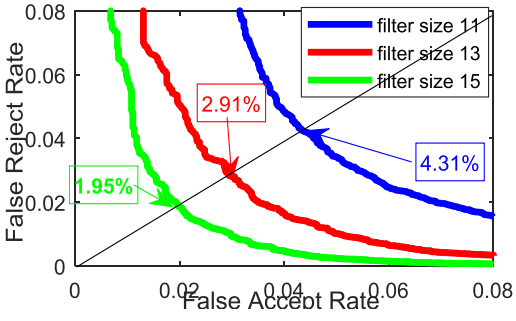

(c)

Fig.6. Results of 11, 13 and 15 BSIF filters with 4 blocks: (a) ROC (b) CMC (c) EER

Table.3. Accuracy and recognition rate for the filters size 11, 13, and 15 with 16 blocks per image

BSIF filter size		**Number of Block *a*×*b***	**Identification**	**Verification**	
K	***n***		**Rank-one**	**V@1 %**	**EER %**
11×11	8	4×4	97.38%	99.05%	0.95%
13×13	8	4×4	96.45%	98.67%	1.20%
15×15	8	4×4	94.95%	97.40%	1.88%

The Table.3 shows the results for the same filters as Table.2 however using a 16 block division per image, thus from Table.3 we can observe that the obtained results are good overall and the best results belongs to filter size 11 with an accuracy at Rank-one of 97.38% and verification accuracy at 1% equals to 99.05% in comparison with other two where BSIF filter size 13 gave an accuracy results at Rank-one of 96.45% and an accuracy of 98.67% for verification rate at 1% while the EER equals to 1.20% as for the BSIF filter size 15 it has the lowest results in comparison with the other two with an accuracy at Rank-one equals to 94.95%

and a verification accuracy at 1% equals to 97.40 % with an EER of 1.88%.

Overall those obtained results can be considered good in comparison to the results obtained from Table.2 using a block division of 4 blocks per image, which proves that the results can get better by dividing and extracting more hiding features within the same image, in addition those results outperform the results obtained from the first experiment.

The Fig.7 shows the results in terms of ROC, CMC and EER curves where this latter represents a comparison study between the filters size 11, 13, and 15 results with a filter length of 8 and number of blocks equals to 16. It can be seen clearly from the Fig.7 that the BSIF filter number 11 outperform the other filters.

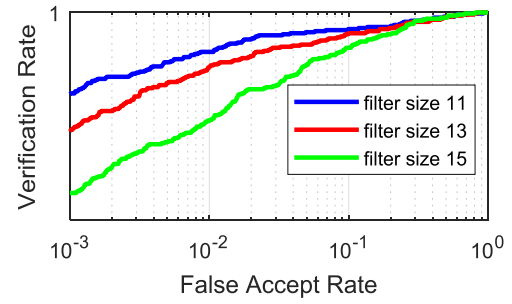

(a)

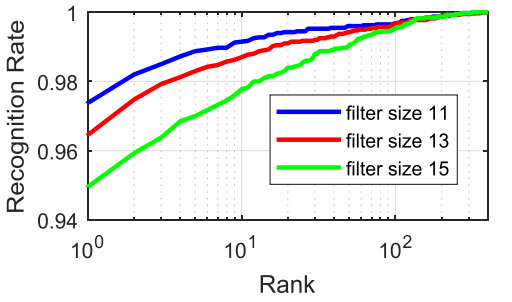

(b)

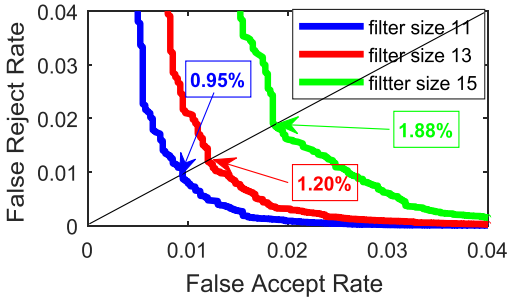

(c)

Fig.7. Results of 11, 13 and 15 BSIF filters with 16 blocks: (a) ROC (b) CMC (c) EER

3.2.3 Experiment III:

The results are introduced in Table.4 for 4 blocks per image, while Table.5 introduce the results for 16 blocks per image.

Table.4. Accuracy and recognition rate for the filter size 17 with different length for 4 blocks per image

BSIF filter size		Number of Block	Identification	Verification	
K	***n***		**Rank-one**	**V@1 %**	**EER %**
17×17	8	2×2	95.88%	98.70%	1.23%
17×17	9	2×2	99.05%	99.88%	0.32%
17×17	**10**	**2×2**	**99.50%**	**99.95%**	**0.18%**
17×17	11	2×2	97.25%	99.30%	0.81%
17×17	12	2×2	98.32%	99.63%	0.55%

The Table.4 shows the results for the BSIF descriptor filter size 17 with several filter length starting from 8, 9, 10, 11 and 12 with a division of 4 blocks per image. The obtained results shows that over all findings are excellent and don't show much big difference between them as the range is higher where it start from 95.88% for the Rank-one with 98.70% for the accuracy verification rate at 1% and EER of 1.23%, those results belongs to the filter size 17 with a length of 8 as for the best results obtained it belongs to filter size 17 with filter length of 8 where it did obtain a 99.50% for Rank-one and a verification accuracy of 99.95% plus 0.18 for EER which is the best result obtained so far, as for the rest of the obtained results of the remaining filter lengths are good as well since they converge toward the best result with a 97.25%, 98.32% and 99.05 % for Rank-one in addition a verification accuracy of 99.30%, 99.63% and 99.88% plus an EER of 0.81%, 0.55% and 0.32%. This experiment was able to outperform the previous experiment even with a block division of 4 blocks per image.

In Fig.8 it shows the results in terms of ROC, CMC and EER curves where this latter represents the results for the filter size 17 with different filter length n (8, 9, 10, 11 and 12) filters size 17 with number of bit equals to 11 results with a filter length of 11 and number of blocks equals to 4. It can be seen clearly from the Fig.8 that the BSIF filter length 11 outperform the other filters.

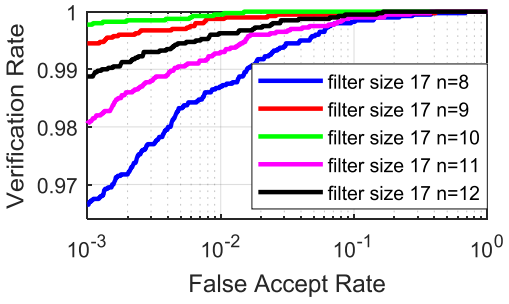

(a)

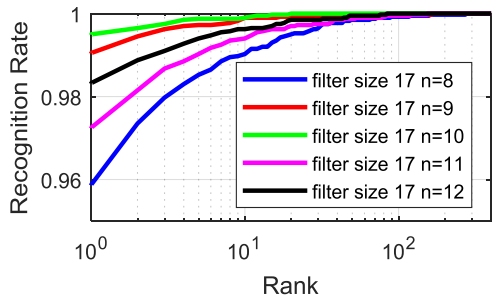

(b)

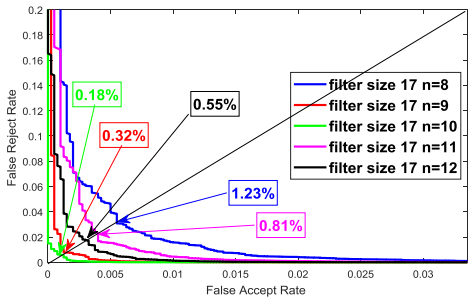

(c)

Fig.8. Results of filter size 17 with filter length: 8, 9, 10, 11 and 12 BSIF filters with 4 blocks: (a) ROC (b) CMC (c) EER

Table.5. Accuracy and recognition rate for the filter size 17 with different length for 16 blocks per image.

BSIF filter size		Number of Block	Identification	Verification	
			Rank-one	V@1 %	EER %
K	***n***				
17×17	8	4×4	93.83%	97.20%	2.00%
17×17	9	4×4	99.05%	99.88%	0.32%
17×17	10	4×4	99.50%	99.95%	0.18%
17×17	11	4×4	99.58%	99.92%	0.15%
17×17	**12**	**4×4**	**99.63%**	**100.00%**	**0.12%**

The Table.5 shows the results for the same filter size (17) as Table.4 however using a 16 block division per image, hence from Table.4 we can observe that overall the obtained results are at the peak and the best by far where we were able to obtain 100% accuracy plus almost all the obtained results are higher than 99% except for filter size 17 length 8 where the results obtained is 93.83% for Rank-one a verification accuracy at 1% of 97.20% and an EER of 2% while the best results is obtained belongs to the filter size 17 with 12 bit length and 16 blocks per image here we were able to get a peak of 99.63% for Rank-one a verification accuracy of 100% and EER of 0.12% as for the remaining results are excellent as well as they range higher than 99%. This experiment was able to outperform all the previous experiment and findings which lead us to the flowing conclusion the best filter size is 17 with filter length 12 bits as for the block division the best is 16 blocks per image.

In Fig.9 it shows the results in terms of ROC, CMC and EER curves where this latter represents the results for the filter size 17 with different filter length n (8, 9, 10, 11 and 12) filters size 17 with number of bit equals to 16 results with a filter length of 11 and number of blocks equals to 16. It can be seen clearly from the Fig.9 that the BSIF filter length 12 outperform the other filters.

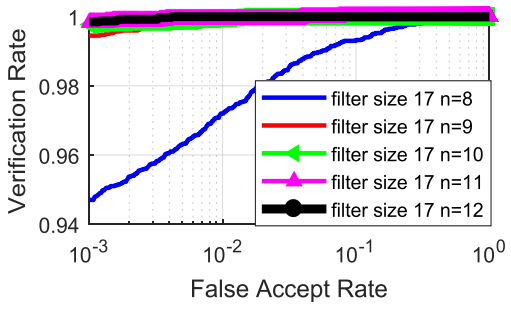

(a)

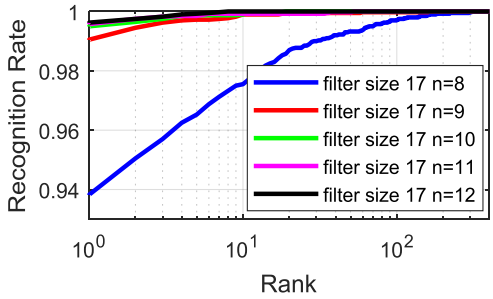

(b)

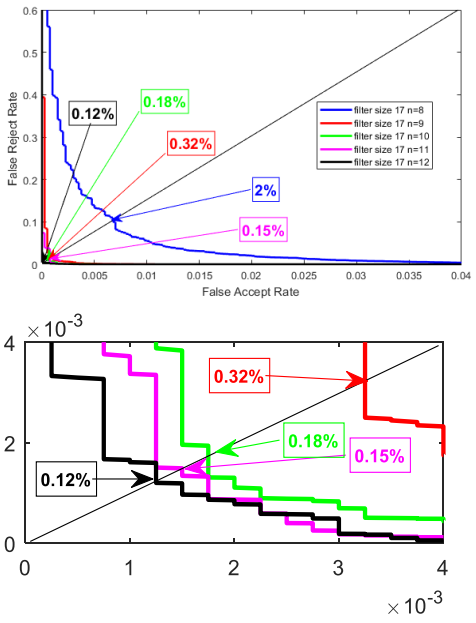

(c)

Fig.9. Results of filter size 17 with filter length: 8, 9, 10, 11 and 12 BSIF filters with 16 blocks: (a) ROC (b) CMC (c) EER

Table.6. Accuracy and recognition rate for the filters size 9, 11, 15 and 17 with different lengths for full image (without block division)

BSIF filter size		Number of Block	Identification	Verification	
			Rank-one	V@1 %	EER %
k	***n***				
9×9	8	1×1	14.63%	17.37%	30.20%
11×11	8	1×1	18.40%	15.40%	33.80%
15×15	8	1×1	54.83%	72.90%	8.88%

17×17	8	1×1	67.07%	75.78%	8.17%

Table.7. Comparative of proposed personal recognition method with the existing approaches

Reference	Method	Identification Rank-1	Verification EER
This paper	TT+BW+BSIF	99.63	0.12%
[6]	MCI+GCI+ST	98.92%	-
[8]	PCA +TPTSR	98.55%	-
[9]	BWFCR	99.15%	-
[13]	Gabor Filters	97.5%	0.0907%
[14]	shape index image and fragile bits	99.75 %	0.281 %
[15]	SSR+PCANet	99.98%	-
[17]	BHF+SCR	99.75%	-

To further proof that a block division is an effective way to extract more relevant features as we dive into the details of the image we conducted this last experiment with a full image without division the results are reported in Table.6.

The Table.6 report the results of the filters size 9, 11, 15 and 17 with filter length 8 our choice for the filter is first the filters with the best obtained results previously as for the length the common used length between them. From Table.6 we can observe that the obtained results don't even get close to the results obtained previously while using the block division where the highest obtained results is 67.07% for Rank-one a verification accuracy of 75.78% and EER of 8.17 for filter size 17 while we obtained with same filter and length using a block division of 4 blocks per image (see Table.4) a Rank-one of 95.88% a verification rate of 98.70% and 1.23% for EER while using 16 blocks per image (see Table. 5) we got a 93.83% for Rank-one a verification accuracy of 97.20% and EER 2% which is by far better than the results obtained while using the whole image. As for the lowest results that can be seen from Table.6 is 14.63% for Rank-one an accuracy of 17.37% for the verification at 1% and an EER of 30.20%, and those results belongs to the filter 9 while with the same condition and using a block per image or 16 blocks per image the difference between the results is way too much (see Table. 1) as the obtained results previously are 97.15% for Rank-one a verification accuracy at 1% is 96.78% and EER of 2.24%.

From the findings overall and from the conducted experiment we can conclude that the use of block division on an image before the feature extraction helps increase the accuracy and gives more relevant features however it has to has one shortcoming which is the expensive computation as more blocks gives better results and take more time.

4. COMPARISON WITH EXISTING STATE OF THE ART 3D PALMPRINT RECOGNITION TECHNIQUES

To validate the effectiveness of the reached results, the following section describe a comparison between the introduced system and some existing systems in the literatures that are given in Table.7. From this Table.our system outperforms the other ones. Including, MCI+GCI+ST method [6], PCA +TPTSR method [8], the block-wise features and collaborative representation (BWFCR) [9] method, Gabor filters+MCI [13], in terms of rank-1 measure. Also, our method is better than shape index image and fragile bits method regarding EER [14]. Except the methods presented in SSR+PCANet [15] and BHF+SCR [17].

5. CONCLUSION

In this paper we have proposed a Block wise 3D palmprint recognition on Tan and Triggs with BSIF descriptor, where we applied Tan and Triggs for pre-processing on 3D palmprint images, and then we divided the images on regular number of blocks followed by a feature extraction phase using BSIF descriptor on the sub images the results were concatenated to obtain one vector for each image, and lastly nearest neighbor classifier was employed in order to classifier the 3D palmprint images. The experiment was conducted in different ways in order to explore the BSIF filters and the different block division numbers and from the obtained results we can say that our system gives good results in comparison too system using the whole image.

REFERENCES

[1] J Engel, "*Epilepsy Studies-Overview*", Elsevier, 2014.
[2] Hae Won Shin, Valerie Jewells, Eldad Hadar, Tiffany Fisher and Albert Hinn, "Review of Epilepsy-Etiology, Diagnostic Evaluation and Treatment", *International Journal of Neurorehabilitation*, Vol. 1, No. 3, pp. 1-6, 2014.
[3] Suruchi Sharma and Vaishali Dixit, "Epilepsy-A Comprehensive Review", *International Journal of Pharma Research and Review*, Vol. 2, No. 12, pp. 61-80, 2013.
[4] Emily L. Johnson, "Seizures and Epilepsy", *Medical Clinics*, Vol. 103, No. 2, pp. 309-324, 2019.
[5] Roland D Thijs and Rainer Surges, "Epilepsy in Adults", *Lancet*, Vol. 24, No. 16, pp. 689-701, 2019.
[6] Hirak Kumar Mukhopadhyay, Chandi Charan Kandar, Sanjay Kumar Das, Lakshmikanta Ghosh and Bijan Kumar Gupta, "Epilepsy and its Management: A Review", *Journal of PharmaSci Tech*, Vol. 1, No. 2, pp. 20-26, 2012.
[7] D. Zhang, G. Lu, W. Li, L. Zhang and N.Luo, "Palmprint Recognition using 3-D Information", *IEEE Transactions on Systems, Man, and Cybernetics, Part C (Applications and Reviews)*, Vol. 39, No. 5, pp. 505-519, 2009.
[8] M.E. Tipping, "The Relevance Vector Machine", *Proceedings of International Conference on Neural Information Processing Systems*, pp. 652-658, 2000.
[9] M.E. Tipping, "Sparse Bayesian Learning and the Relevance Vector Machine", *Journal of Machine Learning Research*, Vol. 1, No. 2, pp. 211-244, 2001.
[10] P. Coutin Churchman, Y. Anez and M. Uzcategui, "Quantitative Spectral Analysis of EEG in Psychiatry Revisited: Drawing Signs Out of Numbers in a Clinical Setting", *Clin Neurophysiology*, Vol. 114, No. 12, pp. 2294-2306, 2003.
[11] D. Zhang, V. Kanhangad, N. Luo and A. Kumar, "Robust Palmprint Verification using 2D and 3D Features", *Pattern Recognition*, Vol. 43, No. 1, pp. 358-368, 2010.

[12] S. Walton, O. Hassan, K. Morgan and M.R. Brown, "A Review of the Development and Applications of the Cuckoo Search Algorithm", *Swarm Intelligence and Bio-Inspired Computation Theory and Applications*, Vol. 25, No. 2, pp. 257-271, 2013.

[13] M. Dorigo, "Optimization, Learning and Natural Algorithms", PhD Dissertation, Department of Computer Science and Engineering, Dipartimento di Elettronica, Politecnico di Milano, pp. 1-145, 1992.

[14] M. Dorigo and Maniezzo V, Colorni, "An Ant System: Optimization by a Colony of Cooperating Agents", *IEEE Transactions on Systems, Man, and Cybernetics Part B: Cybernetics*, Vol. 26, No. 1, pp. 29-41, 1996.

[15] R. Musa, J.P. Arnaout and H. Jung, "Ant Colony Optimization Algorithm to Solve for the Transportation Problem of Cross-Docking Network", *Computers and Industrial Engineering*, Vol. 59, No. 1, pp. 85-92, 2010.

[16] D. Meier, I. Tullumi, Y. Stauffer, R. Dornberger and T. Hanne, "A Novel Backup Path Planning Approach with ACO", *Proceedings of International Conference on Computer and Business Intelligence*, pp. 50-56, 2017.

[17] C. Park, "Epileptic Seizure Detection for Multi-Channel EEG with Deep Convolutional Neural Network", *Proceedings of International Conference on Electronics, Information, and Communication*, pp. 1-8, 2018.

[18] C.M. Bishop, "*Pattern Recognition and Machine Learning*", Springer, 2006.

[19] D.W. Hosmer, S. Lemeshow and R.X. Sturdivant, "*Applied Logistic Regression*", Wiley, 2013.

[20] A. Alkan, E. Koklukaya and A. Subasi, "Automatic Seizure Detection in EEG using Logistic Regression and Artificial Neural Network", *Journal of Neuroscience Methods*, Vol. 148, pp. 167-176, 2005.

[21] A. Subasi, A. Alkana, E. Koklukayab and M.K. Kiymik, "Analysis of Epileptic Seizure Detection Methods based on Parameter Estimation, Power Spectrum Density and Morlet Wavelet Transform", *Neural Networks*, Vol. 18, pp. 985-997, 2005.

[22] X.S. Yang and S. Deb, "Cuckoo Search via Levy Flights", *Proceedings of the World Congress on Nature and Biologically Inspired Computing*, pp. 210-214, 2009.

[23] G. Rodrguez, Generalized Linear Models", Available at: https://data.princeton.edu/wws509/notes/, Accessed at 2018.

[24] K. Deepa and S. Suganya, "A Novel Approach of Segmentation of Cytomegalovirus Image using K-Means Clustering and Discrete Wavelet Transform", *Proceedings of International Conference on Emerging Trends in Information Technology and Engineering*, pp. 341-345, 2020.